Biosensors and Bioelectronics 86 (2016) 1017–1023

Contents lists available at ScienceDirect

Biosensors and Bioelectronics

journal homepage: www.elsevier.com/locate/bios

A cascade amplification approach for visualization of telomerase activity in living cells

Liwen Yan, Jingjing Hui, Yiran Liu, Yuehua Guo, Lu Liu, Lin Ding *, Huangxian Ju

State Key Laboratory of Analytical Chemistry for Life Science, School of Chemistry and Chemical Engineering, Nanjing University, Nanjing, 210023 PR China

ARTICLE INFO

Article history:
Received 11 May 2016
Received in revised form
27 July 2016
Accepted 28 July 2016
Available online 28 July 2016

Keywords:
Telomerase
Living cells
Nanoprobe
Fluorescence imaging
In situ
Catalyzed hairpin assembly

ABSTRACT

An intracellular cascade amplification strategy for ultrasensitive "off-on" imaging of telomerase activity in living cells was designed. The method was based on fabrication of a dual function module-encapsulated liposome nanoprobe, which consisted of a telomerase-targeting responder-transmitter DNA complex (HPT) module and a catalyzed hairpin assembly (CHA) signal amplification module. Upon transfected into living cells, the released HPT could be specifically recognized and extended by telomerase, leading to the release of the transmitter DNA. The transmitter could act as the initiator and catalyzer of CHA amplification, resulting in the lightening up of the reporter complex. The telomerase activity could be monitored in situ by the fluorescence signal without the need for obtaining cell extracts. Because of the recycling use of the transmitter, multiplied enhancement of signal outputs from one extension event was achieved. The proposed strategy could be employed for in situ monitoring of the change of intracellular telomerase activity in response to drugs to detect drug efficacy. Thus the method has great potential in the study of the molecular mechanisms of telomerase-related life processes.

1. Introduction

Telomerase, the telomere-specific reverse transcriptase, is a ribonucleoprotein complex consisting of template RNA and protein (Cech, 2004; Nandakumar et al., 2012; Yu et al., 1990). This holoenzyme allows the maintenance of telomere length by adding tandem telomeric DNA repeats, (TTAGGG)n, at the ends of chromosomes (Ghosh et al., 2012). In normal human tissues, telomerase activity is inhibited, while in 85% of tumors, telomerase activity is reactivated, thus contributing to cellular immortalization and tumor progression (Lingner, 1997; Sauerwald et al., 2013). Therefore, analysis of telomerase activity plays a crucial role in development of novel tumor diagnostic strategies and screening of drugs (Harley, 2008).

The predominant approaches for telomerase detection are based on telomere repeat amplification protocol (TRAP) (Zhou and Xing, 2012), which uses cell extract to obtain telomeric repeat segments followed by different detection techniques (Ding et al., 2016; Ling et al., 2016; Liu et al., 2016; Ohuchida et al., 2004; Sharon et al., 2010; Xiao et al., 2010; Zhang et al., 2014; Zhou et al., 2009). In view of the significance of acquiring spatiotemporal variation of telomerase activity in living cells, the research focus has recently been shifted to developing in situ methods for tracking telomerase activity, which has been achieved through monitoring signals from conformational changes of DNA probes due to primer elongation (Feng et al., 2016; Qian et al., 2013, 2014a, 2014b; Zhuang et al., 2016). However, the improvement in detection sensitivity is still an urgent need.

Inspired by the DNA nature of telomerase primer, the sensitive methods for in situ detection of telomerase activity can be designed by combining the biological function of telomerase with isothermal nucleic acid-based signal amplification. The specificity and predictability of nucleic acid base-pairing provide a rich design space for engineering amplification systems (Bi et al., 2016; Huang et al., 2013, 2015; Li et al., 2011; Ma et al., 2016; Qing et al., 2014; Sternberg and Pierce, 2014; Yin et al., 2008; Zhou et al., 2015). For example, programmable hybridization chain reaction and catalyzed hairpin assembly (CHA) have been used in intracellular microRNA (Cheglakov et al., 2015) and mRNA (Wu et al., 2015a, 2015b) imaging for enhancement of sensitivity. However, to the best of our knowledge, there is no report on using nucleic acid-based signal amplification to facilitate the telomerase imaging inside living cells. The difficulties might lie in two aspects: 1) making a linkage of telomerase extension function with DNA assembly, and 2) specific translation of telomerase activity to a DNA signal without interference from complex intracellular components. To overcome these difficulties, this work developed a cascade approach for visualization of telomerase activity in living cells by linking telomerase-responsive primer extension with CHA-based signal amplification in series through a DNA

* Corresponding author.
E-mail address: dinglin@nju.edu.cn (L. Ding).

http://dx.doi.org/10.1016/j.bios.2016.07.102
0956-5663/

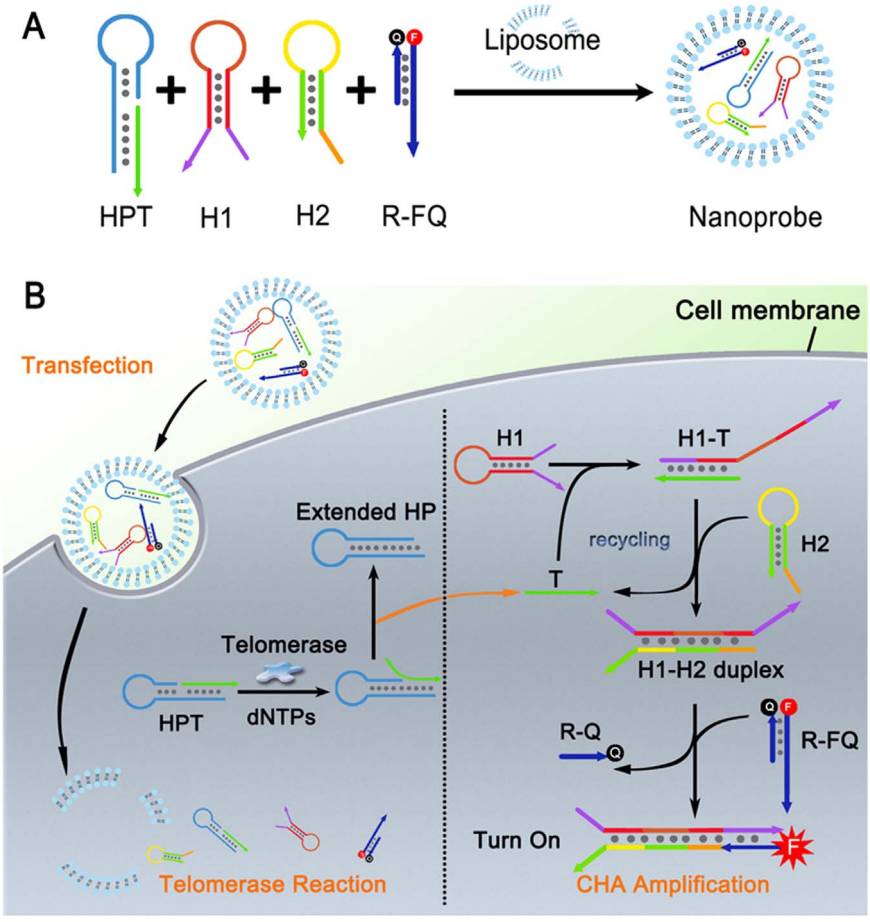

Scheme 1. Schematic illustration of the nanoprobe fabrication (A) and the cascade strategy (B) for visualization of telomerase activity in living cells with enhanced sensitivity.

transmitter (Scheme 1). Compared to existing few reports on in situ telomerase imaging with an equivalent reaction ratio (1:1) (Qian et al., 2014a, 2014b), the proposed strategy achieved multiplied enhancement of signal outputs from one extension event (1: n) because of the recycling use of the transmitter, thus providing a powerful strategy for cell lysis-free, sensitive in situ tracking of telomerase activity.

The proposed strategy relied on the design of a liposome nanoprobe which encapsulated two function modules (Scheme 1). The first was a telomerase-targeting responder-transmitter DNA complex (HPT), a nicked hairpin DNA structure composed of a telomerase primer tagged segment (HP) and a transmitter segment (T) from 5′ to 3′ end that were separated by the nick. The 3′-end of HP along with T was designed to be complementary to the 5′-end of HP, forming the stem part of the hairpin. The sequence of HP was 5′-AACCCT AACCCT AACTCT GCTCGA CGGATT CCCCCCCCCC AATCCG TCGAGC AGAGTT-3′, with the underlined part showing the telomerase primer that can be recognized by telomerase. The second module contained a pair of metastable DNA hairpin (H1, H2), and a hybridized reporter complex (R-FQ) with strands respectively labeled by a fluorophore (F, FAM in this work) and quencher (Q, Dabcyl in this work), thus constituting a catalyzed hairpin assembly (CHA) configuration. Using HeLa cells as the model, upon transfecting the nanoprobe into cytoplasm, the oligonucleotide probes could be released (Scheme 1). In the presence of telomerase and dNTPs, the 3′ end of HP could extend to produce telomeric repeated sequence which was just complementary to 5′ end stem, leading to the displacement of T. The released T could act as the initiator and catalyzer of CHA recycling amplification by hybridizing to the exposed toehold domain of H1. The produced H1-T duplex promoted the generation of H1-H2 duplex followed by the displacement of T for the next catalytic round. H1-H2 could subsequently hybridize with R-F of the reporter complex, leading to the removal of R-Q, thus lightening up the telomerase activity in living cells (Li et al., 2011; Wu et al., 2015a; Yin et al., 2008). Moreover, to ensure sensitive and selective long-term intracellular tracing in real time, locked nucleic acid (LNA) nucleotides were incorporated into the reporter complex, owing to their excellent thermal stability and enzymatic resistance capability in the cell cytoplasm (Kloosterman et al., 2006; Wang et al., 2009).

2. Materials and methods

2.1. Materials and apparatus

Lipofectamine 3000 and P3000 Reagent were obtained from Thermo Fisher Scientific Co. Ltd. (Massachusetts, USA). HeLa cells, DNase I endonuclease and dNTPs were from KeyGen Biotech. Co. Ltd. (Nanjing, China). Gel electrophoresis loading buffer and ladder DNA were purchased from Solarbio. Co. Ltd. (Beijing, China). Epigallocatechingallate (EGCG) was purchased from Sigma-Aldrich Inc. (USA). The nucleic acids were purchased from Takara Clontech & Co. Ltd. (Dalian, China) with the sequences shown in Table S1. Tris buffer solution (pH 7.4) contained 10 mM Tris–HCl, 100 mM NaCl and 5 mM $MgCl_2$. Phosphate buffer saline (PBS, pH 7.4) contained 136.7 mM NaCl, 2.7 mM KCl, 8.72 mM Na_2HPO_4, and 1.41 mM KH_2PO_4. CHAPS lysis buffer contained 10 mM Tris–HCl

(pH 7.5), 1 mM $MgCl_2$, 1 mM ethylenebis (oxyethylenenitrilo) tetraacetic acid (EGTA), 0.1 mM phenylmethanesulfonyl fluoride (PMSF), 0.5% 3-[(3-cholamidopropyl) dimethylammonio] propanesulfonate (CHAPS) and 10% glycerol. All other reagents were of analytical grade. All aqueous solutions were prepared using ultrapure water ($\geq$ 18 MK, Milli-Q, Millipore).

The transmission electron microscopic (TEM) image was obtained on a JEM-2100 transmission electron microscope (JEOL Ltd., Japan). Dynamic light scattering (DLS) was obtained on a 90 Plus/BI-MAS equipment (Brook haven, USA). The UV–vis absorption spectra were obtained with a UV–vis spectrophotometer (Nanodrop-2000C, Nanodrop, USA). Native polyacrylamide gel electrophoresis (PAGE) was performed on a DYCP-31 BN electrophoresis analyzer (Liuyi Instrument Company, China) and imaged on the Bio-Rad ChemDocXRS (USA). Flow cytometric analysis was performed on a Coulter FC-500 flow cytometer (Beckman-Coulter). The fluorescence spectra were obtained on a spectrofluorophotometer (Hitachi F-7000, Japan). The cell images were gained on a TCS SP5 confocal laser scanning microscopy (CLSM) (Leica, Germany).

2.2. Preparation of liposome nanoprobe

HP, H1 and H2 were dissolved in Tris-HCl buffer and annealed over a temperature gradient from 95 to 25 °C in 3 h to form hairpin structures, respectively. Transmitter DNA T (10 μM) and annealed HP (15 μM) were vibrated overnight to form a HPT stock solution (10 μM). R-FQ stock solution (30 μM) was prepared by annealing 30 μM R-F and 45 μM R-Q in Tris-HCl buffer.

For probe preparation, 10 μL oligonucleotide solution containing 1 μM HPT, 10 μM H1, 30 μM H2, 15 μM R-FQ was mixed with 115 μL serum-free cell culture medium containing 4 μL P3000. After incubation for 5 min, 125 μL serum-free culture medium containing 3 μL lipofectamine 3000 was added to the mixture. After 5-min incubation, the solution was filtered by a 100 nm filter membrane to obtain the stock nanoprobe solution. For transfection experiments, 50 μL of stock nanoprobe solution was diluted by 150 μL serum-free cell culture medium to produce the nanoprobe solution, which contained 10 nM HPT, 100 nM H1, 300 nM H2 and 150 nM R-FQ.

Three types of control nanoprobes were also prepared by the same procedure. Random-T and HP were used to replace HPT to mix with the amplification module (final concentration: 100 nM H1, 300 nM H2 and 150 nM R-FQ) for preparation of control nanoprobe I and II, respectively. The control nanoprobe III was prepared by encapsulating 10 nM primer and 150 nM MB in liposome.

2.3. CLSM imaging

HeLa cells were seeded in 20-mm confocal dishes at a density of 1×10^6 mL^{-1} and incubated at 37 °C for 24 h. The medium was then replaced with 200 μL of nanoprobe or control nanoprobe III solution and incubated for different times. After washing the cells by serum-free medium for three times, the fluorescence of cells was visualized with CLSM at stationary parameters including the laser intensity, exposure time and objective lens. The cells were excited at 488 nm and the emission was collected from 500 to 530 nm.

2.4. Monitoring of telomerase activity in HeLa cells upon drug treatment

After seeding HeLa cells (0.5 mL, 1×10^6 mL^{-1}) in 20-mm confocal dishes, 60 μL SODN (10 μM), 60 μL ASODN (10 μM) or 125 μg EGCG were added into the culture medium, respectively. After incubation for 48 h, the cells were washed with serum-free medium for three times and incubated with 200 μL nanoprobe solution for 3 h. Then the cells were washed and observed under CLSM.

3. Results and discussion

3.1. Nanoprobe characterization and feasibility verification in solutions

For probe preparation, to effectively deliver all the oligonucleotide probes into cells, liposome was utilized to serve as the vector owing to its advantages of easy penetration and loading into cells (Gao et al., 2013; Wu et al., 2008). The UV–vis absorption spectrum of the nanoprobe showed a peak at 260 nm illustrating that the oligonucleotide probes had been packaged by the liposome (Fig. S1). The structure and size of the liposome nanoprobe were characterized by transmission electron microscopy (TEM) (Fig. 1A). The average diameter was around 100 nm which was in good agreement with dynamic light scattering (DLS) experiment data (Fig. 1B).

The feasibility of using the responder-transmitter DNA complex HPT to translate the telomerase activity to the amount of released transmitter T was firstly verified by native polyacrylamide gel electrophoresis (PAGE). As shown in Fig. 1C, the complex HPT showed a board band in Lane 3, which moved slower than HP or T alone, demonstrating the formation of complex HPT. After incubating HPT, dNTPs with an extract of HeLa cells for 3 h at 37 °C, the products showed a band located between the bands for HP and HPT, and also a weak band corresponding to T. This result indicated that the primer at the 3′ end of hairpin DNA HPT was extended by telomerase, leading to the release of transmitter T. The HP extension product was estimated to be longer than HP, but still shorter than the original HPT. As a control, in the absence of HeLa extract, neither HP extension product nor released T could be observed after mixing HPT and dNTPs in lysis buffer, demonstrating that the elongation was dependent on telomerase. Next, the trigger of CHA recycling by T was demonstrated by PAGE. As reflected in Fig. 1D, simple mixing of H1 and H2 could not yield new band, demonstrating the absence of cross-interaction between H1 and H2. Upon addition of T, an obvious band was displayed, the location of which was just consistent with the band for annealed product of H1 and H2, suggesting the formation of stable H1-H2 duplex initiated by T.

To verify the T-initiated fluorescence recovery of R-F after CHA, the time course of fluorescence intensity (FI) plot was recorded by incubating the amplification module, i.e. the mixture of H1, H2, R-FP, in the presence/absence of T. The FI gradually elevated with longer incubation time (Fig. S2), while only a weak background signal could be observed in the absence of T. The concentration ratios of oligonucleotide probes play an important role in maximizing the amplification, thus were optimized in vitro. At a constant H1 concentration of 100 nM, the concentration of H2 and R-FQ were respectively optimized to be 300 and 150 nM (Fig. S3), which were used for both in vitro and living cell experiment. The 2-fold excess of H2 concentration over H1 contributed to the driving of equilibrium of the CHA to yield more H1-H2 duplex (Wu et al., 2015a).

To demonstrate the T-dependent recovery of fluorescence signal after CHA, different concentrations of T were subjected to initiate the CHA. With increasing concentration of T (c_T), the fluorescence emission peaked at 518 nm elevated (Fig. 1E). The relative FI (FI′) showed a linear relationship with c_T in the range of 1–15 nM. The fitted equation is $FI' = 0.985 + 0.327c_T$ (Fig. 1F). To analyze the telomerase activity in cancer cells in vitro by the capability to produce T, different amounts of HeLa cell extract

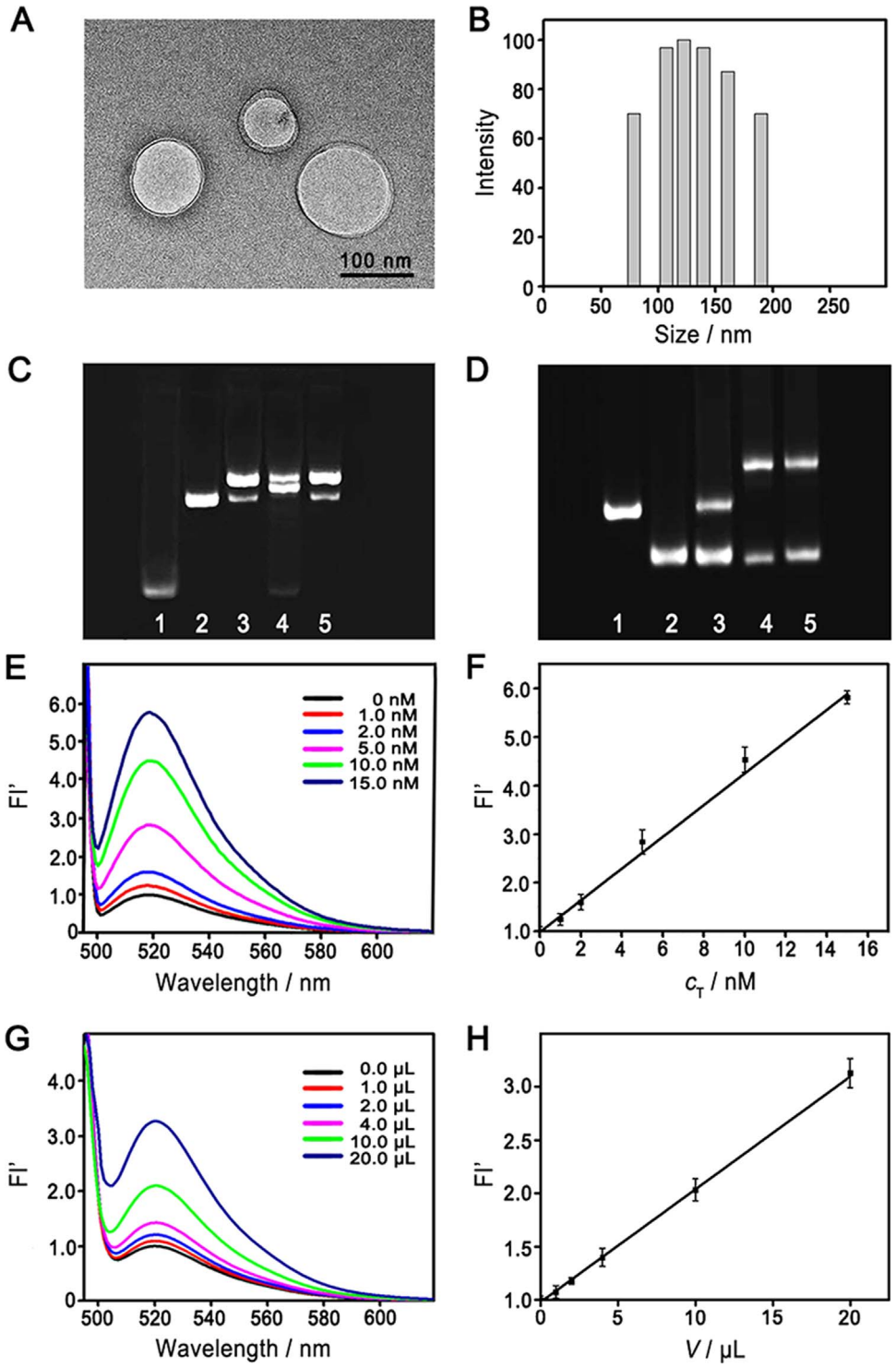

Fig. 1. (A) TEM image and (B) DLS characterization of the nanoprobe. (C) PAGE image of T (Lane 1), HP (Lane 2), HPT (Lane 3), and HPT after incubation with dNTPs in the presence (Lane 4) and absence (Lane 5) of HeLa extract. (D) PAGE image of H1 (Lane 1), H2 (Lane 2), mixture of H1 and H2 (Lane 3), annealed H1 and H2 (Lane 4) and the mixture of H1, H2 and T (Lane 5). (E) Fluorescence spectra of the amplification module containing 100 nM H1, 300 nM H2 and 150 nM R-FQ after incubation with T of various concentrations (0, 1, 2, 5, 10, 15 nM). (F) Plot of relative fluorescence intensity (FI′) vs. concentration of T (c_T). FI′ was calculated as follows: $FI' = FI/FI_0$, where FI_0 was the fluorescence intensity without sample added. (G) Fluorescence spectra of the mixture of HPT and the amplification module after incubation with various volumes of HeLa extract (0, 1, 2, 4, 10, 20 μL). (H) Plot of FI′ vs. volume of cell extract (V).

were subjected to incubate with the mixture of HPT and the amplification module for 3 h. The FI′ was found to be linear to the cell extract volume (V) with an equation of $FI' = 0.979 + 0.106V$ (Fig. 1G and H). Taking the two equations together, the average telomerase activity in a single cell was estimated to produce 2.5×10^{-19} mol T.

To evaluate the stability of the developed platform, the time course of FI plot was recorded by incubating the mixture of HPT and the amplification module in the presence/absence of telomerase-contained cell lysis in various solutions, including Tris buffer of pH 7.4, cell culture medium DMEM and water (Fig. S4). The variation tendency of fluorescence in DMEM was similar as that in Tris buffer, suggesting that the influence of the components

in culture medium to the stability of the developed platform could be ignored. While, the recovery of fluorescence was less effective in water due to the lack of salt ions necessary for the HP extension and DNA hybridization reaction. Next we investigated the resistance of the nucleic acid mixture in degrading enzyme-contained acidic environments (pH 6.0) using endonuclease DNase I as the model. Negligible fluorescence signal could be observed upon addition of DNase I due to the good resistance capability of LNA, which suggested the stability of the proposed platform in the subcellular environment with various digesting nucleases.

3.2. *In situ imaging of cellular telomerase activity and specificity verification*

Having demonstration of the capability of the proposed strategy for analysis of telomerase activity in cell extract, the feasibility of using the liposome nanoprobe for tracing telomerase in living cells was studied. Lipofectamine 3000, as a new generation of transfection agent with lower cellular toxicity, was used to complex with the nucleic acid probes and efficiently carry them into cells, which could be released upon internalization. The formation of the complex relies on the stoichiometric binding between the

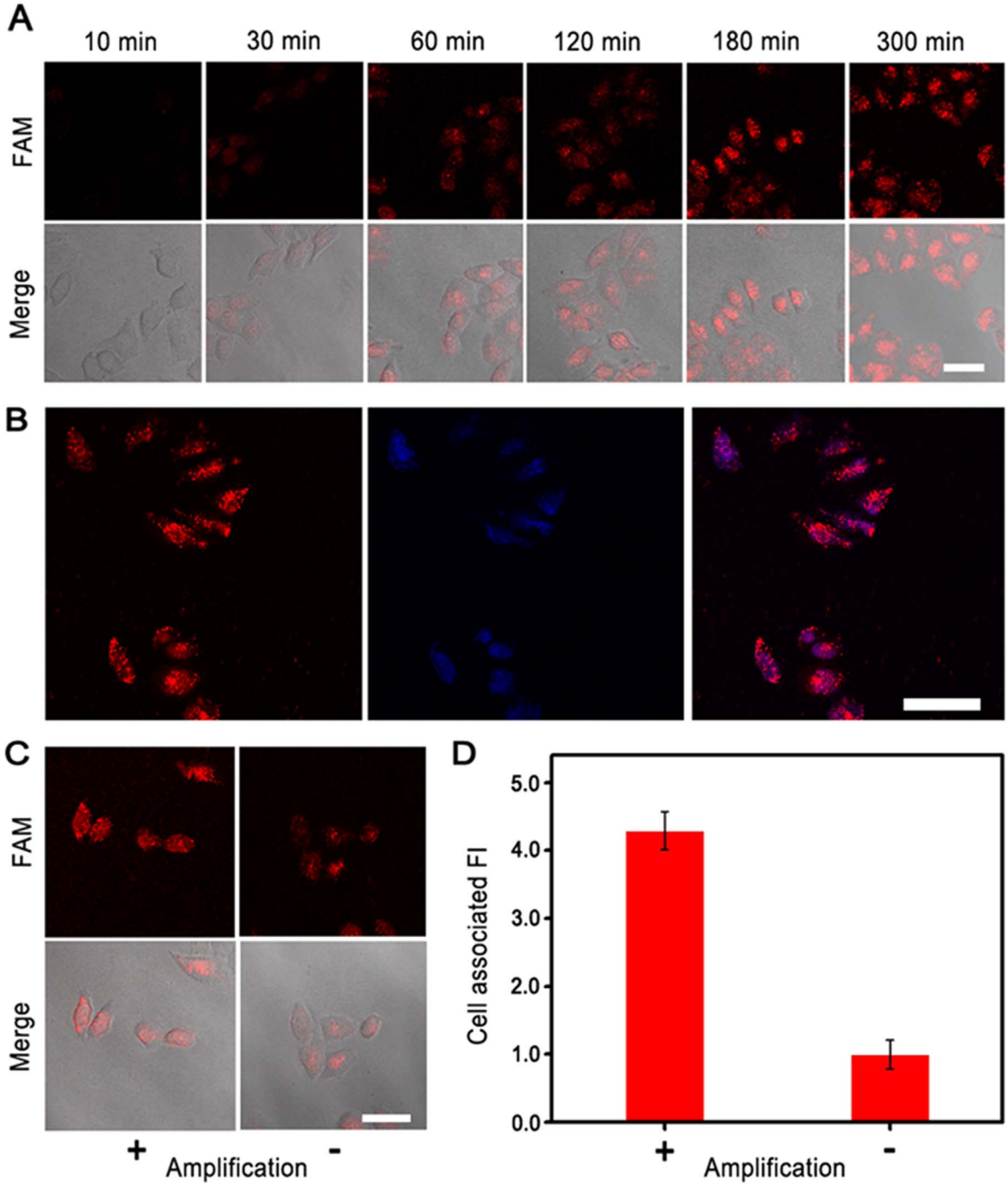

Fig. 2. (A) Time course of confocal images of HeLa cells after incubation with the nanoprobe. (B) Co-staining of HeLa cells by nanoprobe (Red) and nuclear dye DAPI (Blue). CLSM imaging (C) and flow cytometric analysis (D) of HeLa cells after incubation with nanoprobe (amplification +) or control nanoprobe III (amplification −). Scale bars: 50 μm.

positively charged head group (usually containing nitrogen atoms) of a lipid and the negatively charged sugar-phosphate backbone of a nucleic acid molecule (Dalby et al., 2004), resulting in the packing of several DNA strands together within the lipid bilayer (Gershon et al., 1993). Thus it could be reasonably hypothesized that this stochastic encapsulation process was independent of the sequence of nucleic acids, and a certain ratio of DNA strands should be encapsulated in each liposome. The recovery of fluorescence signal of FAM in living HeLa cells was tracked in real time by confocal fluorescence imaging (Fig. 2A). After 30-min incubation, weak fluorescence could be observed inside cell, then the intensity rose with increasing incubation time and reached a plateau at 180 min. The observed bright fluorescence could be attributed to the telomerase-triggered T release, the following T-initiated CHA amplification and recovery of FAM fluorescence, thus reflecting the telomerase activity inside living cells. The location of the recovered FAM fluorescence was found to be distributed throughout the cells, as reflected by comparing FAM signals with the blue fluorescence from DAPI staining of cell nucleus (Fig. 2B). The specificity of the nanoprobe was validated by two control experiments (Fig. S5). To verify the telomerase-triggered T release in living cells, a DNA hairpin (Random-T) composed of a random segment and T segment was used to replace HPT to fabricate the control nanoprobe I for imaging experiment. Only negligible fluorescence could be observed, suggesting that the displacement of T relied on the specific recognition of telomerase toward HP sequence. Next, control nanoprobe II using HP segment without T to replace HPT was employed for demonstrating the T-specific signal amplification. The obvious weak signal indicated that there was almost no cross interaction between H1 and H2 in the absence of T. These two control experiments also demonstrated the stability of the reporter complex owing to LNA incorporation (Kloosterman et al., 2006; Wang et al., 2009).

3.3. Demonstration of the amplification efficacy

To demonstrate the 1:n amplification efficacy of the proposed nanoprobe for tracing telomerase activity, a control nanoprobe III with 1:1 output-input ratio was constructed for comparison. This liposome nanoprobe contained a MB and the primer, and the former could be opened by telomerase-expended primer product to yield fluorescence signal. As reflected in Fig. 2C, the CHA amplified fluorescence signal obtained by the nanoprobe was about 4.0-fold of the control nanoprobe III using equivalent primer concentration by confocal fluorescence imaging. The amplification ratio was also verified by flow cytometric assay to exclude the possible individual difference (Fig. S6), and the mean fluorescence signal from the nanoprobe was 4.3-fold of the control nanoprobe III (Fig. 2D), thus verifying the signal amplification capability of the proposed nanoprobe for imaging telomerase activity. These results also demonstrated that the proposed detection platform overcame the limitation of "using nucleic acid-based signal amplification to detect nucleic acids" in the field of intracellular sensing.

3.4. In situ monitoring of the dynamic changes of telomerase activity

The high sensitivity of the proposed strategy facilitated in situ monitoring of dynamic changes of telomerase activity in response to a series of drugs. Telomerase sense oligodeoxynucleotide (SODN), telomerase antisense oligodeoxynucleotide (ASODN), and epigallocatechingallate (EGCG) were used as model drugs to inhibit telomerase activity in HeLa cells. After incubating HeLa cells with ASODN, SODN and EGCG, respectively, for 48 h, the nanoprobe was added to cell culture medium. Obvious lower fluorescence signals were observed (Fig. 3), suggesting the inhibition effect of these drugs. Through comparing the signals from the three drugs, EGCG displayed the strongest effect. These results suggested that this work proposed a potential strategy for screening of telomerase-targeting drugs. In addition, this result also demonstrated the specificity of the nanoprobe. For cells with suppressive telomerase activity, only weak fluorescence could be observed, suggesting that the observed signal without drug treatment (Fig. 2A) was exactly due to telomerase-mediated signal generation rather than other DNA polymerases.

4. Conclusions

In conclusion, this work designed a cascade strategy to link telomerase-triggered primer elongation with oligonucleotide-based signal amplification by a transmitter DNA for ultrasensitive "off-on" imaging of telomerase activity in living cells. All the

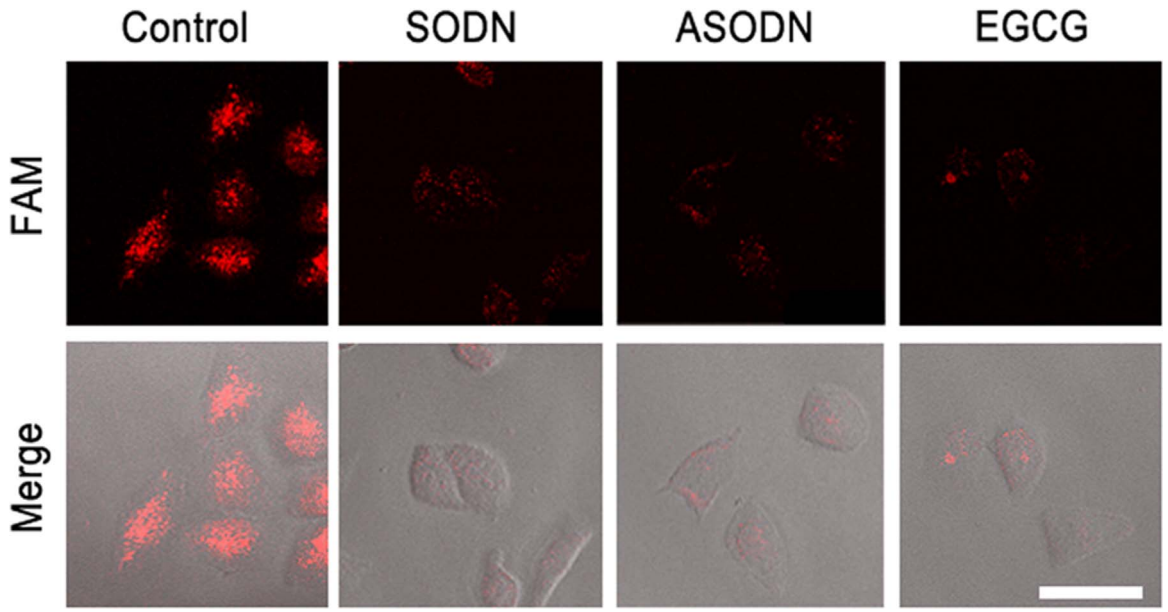

Fig. 3. Confocal images of untreated HeLa cells (control) and HeLa cells pretreated with SODN, ASODN and EGCG, respectively, after incubation with the nanoprobe for 3 h. Scale bar: 50 μm.

oligonucleotide probes were wrapped in liposome to produce a nanoprobe for assisting cellular delivery. The transmitter DNA, released by primer extension could act as the initiator and catalyser of the CHA amplification, thus the proposed strategy achieved multiplied enhancement of signal outputs. The proposed strategy was further employed for monitoring the change of intracellular telomerase activity in response to drugs to detect drug efficacy. It can be anticipated that the method can be also used to compare telomerase activity among different cell lines as well as differentiate normal cells from tumor cells. We believe that the proposed strategy offers a new paradigm for fabrication of sensitive and specific detection platform in living cells, and could contribute to the acquirement of deep insight into the molecular mechanisms of telomerase-related life processes.

Acknowledgements

We gratefully acknowledge National Natural Science Foundation of China (21322506, 21135002) and National Basic Research Program (2014CB744501).

Appendix A. Supplementary material

Supplementary data associated with this article can be found in the online version at http://dx.doi.org/10.1016/j.bios.2016.07.102.

References

Bi, S., Ye, J.Y., Dong, Y., Li, H.T., Cao, W., 2016. Chem. Commun. 52, 402–405.
Cech, T.R., 2004. Cell 116, 273–279.
Cheglakov, Z., Cronin, T.M., He, C., Weizmann, Y., 2015. J. Am. Chem. Soc. 137, 6116–6119.
Dalby, B., Cates, S., Harris, A., Ohki, E.C., Tilkins, M.L., Price, P.J., Ciccarone, V.C., 2004. Methods 33, 95–103.
Ding, C.F., Li, X.Q., Wang, W., Chen, Y.Y., 2016. Biosens. Bioelectron. 83, 102–105.
Feng, Q.M., Zhu, M.J., Zhang, T.T., Xu, J.J., Chen, H.Y., 2016. Analyst 141, 2474–2480.
Gao, W.W., Hu, C.M.J., Fang, R.H., Zhang, L.F., 2013. J. Mater. Chem. B 1, 6569–6585.
Gershon, H., Ghirlando, R., Guttman, S.B., Minsky, A., 1993. Biochemistry 32, 7143–7151.
Ghosh, A., Saginc, G., Leow, S.C., Khattar, E., Shin, E.M., Yan, T.D., Wong, M., Zhang, Z. Z., Li, G.L., Sung, W.K., Zhou, J.B., Chng, W.J., Li, S., Liu, E., Tergaonkar, V., 2012. Nat. Cell Biol. 14, 1270–1281.
Harley, C.B., 2008. Nat. Rev. Cancer 8, 167–179.
Huang, F.J., You, M.X., Han, D., Xiong, X.L., Liang, H.J., Tan, W.H., 2013. J. Am. Chem. Soc. 135, 7967–7973.
Huang, Y., Liu, X.Q., Huang, H.K., Qin, J., Zhang, L.L., Zhao, S.L., Chen, Z.F., Liang, H., 2015. Anal. Chem. 87, 8107–8114.
Kloosterman, W.P., Wienholds, E., Bruijn, E., Kauppinen, S., Plasterk, R.H.A., 2006. Nat. Methods 3, 27–29.
Li, B.L., Andrew, D.E., Chen, X., 2011. Nucleic Acids Res 39 (16), e110.
Ling, P.H., Lei, J.P., Jia, L., Ju, H.X., 2016. Chem. Commun. 52, 1226–1229.
Lingner, J., 1997. Science 276, 561–567.
Liu, Y.J., Wei, M., Liu, X., Wei, W., Zhao, H.Y., Zhang, Y.J., Liu, S.Q., 2016. Chem. Commun. 52, 1796–1799.
Ma, C., Liu, H.Y., Tian, T., Song, X.R., Yu, J.H., Yan, M., 2016. Biosens. Bioelectron. 83, 15–18.
Nandakumar, J., Bell, C.F., Weidenfeld, I., Zaug, A.J., Leinwand, L.A., Cech, T.R., 2012. Nature 492, 285–289.
Ohuchida, K., Mizumoto, K., Ishikawa, N., 2004. Cancer 101, 2309–2317.
Qian, R.C., Ding, L., Ju, H.X., 2013. J. Am. Chem. Soc. 135, 13282–13285.
Qian, R.C., Ding, L., Yan, L.W., Lin, M.F., Ju, H.X., 2014a. J. Am. Chem. Soc. 136, 8205–8208.
Qian, R.C., Ding, L., Yan, L.W., Lin, M.F., Ju, H.X., 2014b. Anal. Chem. 86, 8642–8648.
Qing, Z.H., He, X.X., Huang, J., Wang, K., Zou, Z., Qing, T.P., Mao, Z.G., Shi, H., He, D.G., 2014. Anal. Chem. 86, 4934–4939.
Sauerwald, A., Sandin, S., Cristofari, G., Scheres, S.H.W., Lingner, J., Rhodes, D., 2013. Nat. Struct. Mol. Biol. 20, 454–460.
Sharon, E., Freeman, R., Riskin, M., Gil, N., Tzfati, Y., Willner, I., 2010. Anal. Chem. 82, 8390–8397.
Sternberg, J.B., Pierce, N.A., 2014. Nano Lett. 14, 4568–4572..
Wang, K., Tang, Z., Yang, C., Kim, Y., Fang, X., Li, W., Wu, Y., Colin, D., Cao, Z., Li, J., Colon, P., Lin, H., Tan, W., 2009. Angew. Chem. Int. Ed. 48, 856–870.
Wu, C.C., Cansiz, S., Zhang, L.Q., Teng, I.T., Qiu, L.P., Li, J., Liu, Y., Zhou, C.S., Hu, R., Zhang, T., Cui, C., Cui, L., Tan, W.H., 2015a. J. Am. Chem. Soc. 137, 4900–4903.
Wu, G.H., Mikhailovsky, A., Khant, H.A., Fu, C., Chiu, W., Zasadzinski, J.A., 2008. J. Am. Chem. Soc. 130, 8175–8177.
Wu, Z., Liu, G.Q., Yang, X.L., Jiang, J.H., 2015b. J. Am. Chem. Soc. 137, 6829–6836.
Xiao, Y., Dane, K.Y., Uzawa, T., Csordas, A., Qian, J.R., Soh, H.T., Daugherty, P.S., Lagally, E.T., Heeger, A.J., Plaxco, K.W., 2010. J. Am. Chem. Soc. 132, 15299–15307.
Yin, P., Choi, H.M.T., Calvert, C.R., Pierce, N.A., 2008. Nature 451, 318–322.
Yu, G.L., Bradley, J.D., Attardi, L.D., Blackburn, E.H., 1990. Nature 344, 126–132.
Zhang, H.R., Wang, Y.Z., Wu, M.S., Feng, Q.M., Shi, H.W., Chen, H.Y., Xu, J.J., 2014. Chem. Commun. 50, 12575–12577.
Zhou, X.M., Xing, D., Zhu, D.B., Jia, L., 2009. Anal. Chem. 81, 255–261.
Zhou, X.M., Xing, D., 2012. Chem. Soc. Rev. 41, 4643–4656.
Zhou, W.J., Liang, W.B., Li, X., Chai, Y.Q., Yuan, R., Xiang, Y., 2015. Nanoscale 7, 9055–9061.
Zhuang, Y., Huang, F.J., Xu, Q., Zhang, M.S., Lou, X.D., Xia, F., 2016. Anal. Chem. 88, 3289–3294.